Available online at www.sciencedirect.com
ScienceDirect
Polymer 48 (2007) 7017–7028
polymer
www.elsevier.com/locate/polymer

Poly(D,L-lactide)/poly(methyl methacrylate) interpenetrating polymer networks: Synthesis, characterization, and use as precursors to porous polymeric materials

Géraldine Rohman, Françoise Lauprêtre, Sylvie Boileau, Philippe Guérin, Daniel Grande*

Equipe "Systèmes Polymères Complexes", Institut de Chimie et des Matériaux Paris-Est, UMR 7182 CNRS – Université Paris XII-Val-de-Marne, 2, rue Henri Dunant, 94320 Thiais, France

Received 22 May 2007; received in revised form 18 September 2007; accepted 30 September 2007
Available online 5 October 2007

Abstract

The use of semi-hydrolyzable oligoester-derivatized interpenetrating polymer networks (IPNs) as nanostructured precursors provides a straightforward and versatile approach toward mesoporous networks. Different poly(D,L-lactide) (PLA)/poly(methyl methacrylate) (PMMA)-based IPNs were synthesized by resorting to the so-called *in situ* sequential method. The PLA sub-network was first generated from a dihydroxy-telechelic PLA oligomer *via* an end-linking reaction with Desmodur® RU as a triisocyanate cross-linker. Subsequently, the methacrylic sub-network was created by free-radical copolymerization of methyl methacrylate (MMA) and a dimethacrylate (either bisphenol A dimethacrylate or diurethane dimethacrylate) with varying compositions (initial MMA/dimethacrylate composition ranging from 99/1 to 90/10 mol%). Both cross-linking processes were monitored by real-time infrared spectroscopy. The microphase separation developed in IPN precursors was investigated by differential scanning calorimetry (DSC). Furthermore, the quantitative hydrolysis of the PLA sub-network, under mild basic conditions, afforded porous methacrylic structures with pore sizes ranging from 10 to 100 nm –at most– thus showing the effective role of cross-linked PLA sub-chains as porogen templates. Pore sizes and pore size distributions were determined by scanning electron microscopy (SEM) and thermoporometry *via* DSC measurements. The mesoporosity of residual networks could be attributed to the good degree of chain interpenetration associated with both sub-networks in IPN precursors, due to their peculiar interlocking framework.

Keywords: Interpenetrating polymer networks; Poly(D,L-lactide); Porous materials

1. Introduction

Interest in the design of porous polymeric materials originates from the large variety of applications in which they are involved, *e.g.* monoliths for chromatographic techniques, separation membranes, interlayer dielectrics, high surface area catalytic supports, as well as size/shape-selective nanoreactors [1–6]. In addition to the classical synthetic strategies based on the use of simple porogens such as solvents or gases, original approaches using suitable porogen templates have emerged: such templates are able to induce specific structural pores within the residual structures. These template-oriented routes are quite interesting as a wide array of porous polymers with a well-defined porosity can be derived therefrom [7,8]. Some elegant methodologies include molecular imprinting [9,10], removal of self-assembled molecules from supramolecular architectures [11], selective destruction of one block in self-organized block copolymers [12–20], and selective thermal or photochemical degradation of a thermoplastic polymer homogeneously blended within a thermostable polymer matrix [21–23]. Even though semi-degradable block copolymers are arguably ideal precursors for the formation of ordered mesoporous systems, the relatively poor mechanical, thermal, and chemical stability of un-cross-linked polymer structures entails that cross-linking of the remaining block in the residual porous matrices generally appears to be crucial to get access to some of the aforementioned applications.

* Corresponding author. Tel.: +33 (0)1 49 78 11 77; fax: +33 (0)1 49 78 12 08.
E-mail address: grande@glvt-cnrs.fr (D. Grande).

0032-3861/$ - see front matter © 2007 Elsevier Ltd. All rights reserved.
doi:10.1016/j.polymer.2007.09.044

An alternative strategy for engineering porous cross-linked materials has been put forward only by a handful number of research teams *via* the use of interpenetrating polymer networks (IPNs) as precursors [24–26]. IPNs are generally defined as a combination of two independent polymers in a network form, at least one of which has been synthesized in the presence of the other [27]. Due to their interlocking framework, macrophase segregation is prevented, and the spatial scale of phase separation may be restricted to domain sizes of a few hundreds or even tens of nanometers. It is noteworthy that IPN morphology is mainly governed by the interplay between two types of competitive factors: thermodynamic ones, *i.e.* intermolecular interactions between both partners, *versus* kinetic ones, *i.e.* competition between cross-linking and phase separation. Hence, the microphase-separated morphologies developed in IPNs can be synthetically controlled by the proper selection of component nature and composition, as well as polymerization kinetics and mechanisms. Such complex polymer structures are of particular interest when they arise from the association of two components that exhibit a contrasted degradability under specific conditions. Indeed, (meso)porous networks can be generated from such IPNs by resorting to selective degradation methods [24–26].

The first porous polymers were derived from sequential IPNs based on polystyrene (PS) and poly(*n*-butyl acrylate) (PBA) with various compositions in which the latter sub-network contained labile cross-links resulting from acrylic acid anhydride and the PS sub-network contained stable cross-links arising from divinylbenzene [24]. De-cross-linking of the PBA-based sub-network was accomplished by selectively hydrolyzing the labile cross-links under mild basic conditions, thus leading to the formation of PS-based porous networks. Du Prez and Goethals [25] reported the synthesis of porous sequential IPNs prepared by the copolymerization of an acrylate-terminated poly(1,3-dioxolane) bismacromonomer with methyl (meth)acrylate, followed by copolymerization of methyl (meth)acrylate and tetraethylene glycol diacrylate. The poly(1,3-dioxolane) segments were degraded under strong acidic conditions, thus affording residual porous poly(meth)acrylate networks. It should be stressed that in both studies the primary aim was not the preparation of porous materials; the main purpose was actually the development of an approach to get an insight into the morphologies of IPNs. Electron beam irradiation is another interesting method for pore generation from IPNs, as reported by Pionteck for IPN-like structures based on polyethylene (PE) and poly(methyl methacrylate-*co*-butyl methacrylate) [26]. Partial decomposition of the polymethacrylate partner was achieved by using an irradiation dose of 800 kGy, while further cross-linking the PE sub-network. This "selective" degradation resulted in an open porous PE structure, thus providing a new way to get access to polymer membranes useful for micro- or ultra-filtration.

Accordingly, it is obvious that detailed studies on (meso)porous polymers derived from IPNs remain scarce. In this context, our group has undertaken a thorough investigation of the scope and limitations associated with the utilization of two types of reference systems for the design of (meso)porous cross-linked materials. We have recently reported the straightforward and effective preparation of (meso)porous networks with tunable pore sizes from semi-IPNs constituted of uncross-linked oligoesters entrapped in a "rigid" sub-network [28]. In continuation of the latter work, the present paper focuses on the synthetic strategy developed to get access to (meso)porous networks using poly(D,L-lactide) (PLA)/poly(methyl methacrylate) (PMMA)-based IPNs as nanostructured precursors. After describing the synthesis of such IPNs through the so-called *in situ* sequential method [29], the kinetics of the cross-linking processes involved in network formation is examined by real-time infrared spectroscopy. To gain an insight into the microphase separation developed in the systems considered, a differential scanning calorimetry (DSC) investigation is also performed. Then, by taking advantage of the well-known hydrolytic degradability of PLA, mesoporous methacrylic networks can be generated from the semi-hydrolyzable IPNs upon hydrolysis of the PLA sub-network, under mild basic conditions. The dependence of the porosity associated with the resulting networks on two structural parameters, namely the cross-link density of the PMMA sub-network and the nature of the corresponding cross-linker, is particularly investigated. Pore sizes and pore size distributions are determined by scanning electron microscopy (SEM) and thermoporometry using DSC.

2. Experimental section

2.1. Materials

Dihydroxy-telechelic PLA (M_n (^{1}H NMR) = 1700 g mol^{-1}; M_w/M_n (SEC) = 1.2) was synthesized by ring-opening polymerization of D,L-lactide initiated by the ethylene glycol/tin(II) octanoate system, as previously described [30]. Dibutyltin dilaurate (DBTDL, Fluka) was used as received. 4,4′,4″-Triisocyanato-triphenylmethane (Desmodur® RU, 1.25 mol L^{-1} in dichloromethane solution) was provided by Bayer. Methyl methacrylate (MMA, Aldrich) was dried over CaH_2, and distilled under vacuum prior to use. Bisphenol A dimethacrylate (BADMA) and diurethane dimethacrylate (DUDMA) were purchased from Aldrich and used as received. AIBN (Merck) was purified by recrystallization in methanol.

2.2. Network synthesis

2.2.1. PLA single network

A PLA single network was typically prepared as follows by using $[NCO]_0/[OH]_0$ and $[DBTDL]_0/[PLA]_0$ ratios of 1.4 and 0.44, respectively. One gram (5.9×10^{-4} mol) of PLA was dissolved in 0.91 mL (1.21 g) of dichloromethane and subsequently, 0.45 mL (0.21 g, 5.6×10^{-4} mol) of Desmodur® RU and 0.15 mL (2.5×10^{-4} mol) of DBTDL were added under nitrogen. The solution was poured under nitrogen into a mold which consisted of two glass plates clamped together and separated by a 2-mm thick silicone rubber gasket. After 20 h at room temperature, the mold was kept at 65 °C for

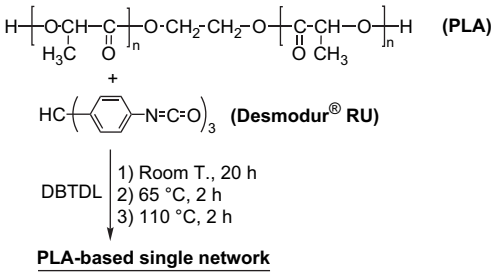

Fig. 1. Preparation of PLA-based single network.

2 h, and the reaction medium was finally cured at 110 °C for 2 h (Fig. 1).

2.2.2. PMMA single networks

Typically, a single network with a MMA/DUDMA molar composition of 90/10 mol% was prepared as follows. A homogeneous mixture of MMA (0.9 g, 9×10^{-3} mol), DUDMA (0.47 g, 10^{-3} mol), and AIBN (0.033 g, 2×10^{-4} mol, $[AIBN]_0/([MMA]_0 + 2[DUDMA]_0) = 0.02$) was degassed under vacuum, and poured under nitrogen into a mold, as in the previous case. The mold was then kept at 65 °C for 2 h, and the reaction medium was finally cured at 110 °C for 2 h (Fig. 2).

2.2.3. PLA/PMMA IPNs

A standard synthesis of an IPN with a PLA/PMMA mass composition of 50/50 wt% and a MMA/DUDMA molar composition of 90/10 mol% is described next. One gram (5.9×10^{-4} mol) of PLA, 0.76 g (7.6×10^{-3} mol) of MMA, 0.40 g (8.5×10^{-4} mol) of DUDMA, and 0.028 g (1.7×10^{-4} mol) of AIBN ($[AIBN]_0/([MMA]_0 + 2[DUDMA]_0) = 0.02$) were mixed homogeneously in a flask and degassed under vacuum. A 0.45 mL (0.21 g, 5.6×10^{-4} mol) of Desmodur® RU and 0.15 mL (2.5×10^{-4} mol) of DBTDL were then added under nitrogen in a glove box. Subsequently, the solution was introduced under nitrogen into a mold. After 20 h at room temperature, the mold was then placed in an oven operating at 65 °C. After 2 h, the temperature was raised to 110 °C for a 2 h of curing. It is noteworthy that the $[NCO]_0/[OH]_0$ and $[DBTDL]_0/[PLA]_0$ ratios were constant and equal to 1.4 and 0.44, respectively.

Other PMMA single networks and IPNs are synthesized in similar ways by changing the dimethacrylate nature (DUDMA or BADMA) and/or the initial MMA/dimethacrylate molar composition (90/10, 97/3, 95/5, or 99/1 mol%), as depicted in Figs. 2 and 3, respectively.

2.2.4. Network extraction

To remove the sol fractions and determine their amounts, all networks were subjected to a Soxhlet extraction with dichloromethane for 24 h. The recovered sol fractions (after removing the solvent using a rotary evaporator) and extracted networks were dried under vacuum, and weighed prior to further analyses. The amounts of sol fractions were calculated as the mass percentages of extractables.

2.3. Formation of porous networks by PLA hydrolysis from IPNs

A network sample (0.2 g) was immersed at 60 °C, in different vials containing 4 mL of a phosphate buffer aqueous solution (5×10^{-2} mol L^{-1} KH_2PO_4, 4.9×10^{-2} mol L^{-1} NaOH, pH = 8.2) and 4 mL of ethanol. After a given period of time, the reaction medium was neutralized by a 0.1 mol L^{-1} NaOH aqueous solution, and the residual network was rinsed with distilled water up to neutral pH. The sample was finally dried under vacuum, and weighed prior to further analyses.

The total hydrolysis of the PLA sub-network from IPNs thus led to the formation of residual porous methacrylic networks (Fig. 3).

2.4. Instrumentation

^{1}H NMR spectra of sol fractions and hydrolysis products were recorded at room temperature using a Bruker AC 200 spectrometer operating at a resonance frequency of 200 MHz. The sample concentration was 10 mg mL^{-1}, and $CDCl_3$ was used as the solvent and internal standard (7.27 ppm). High-resolution solid-state ^{13}C NMR spectra of networks were obtained at a

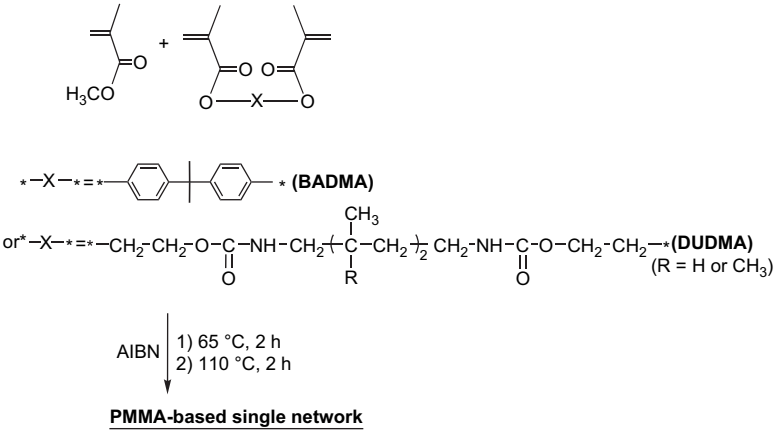

Fig. 2. Preparation of PMMA-based single networks.

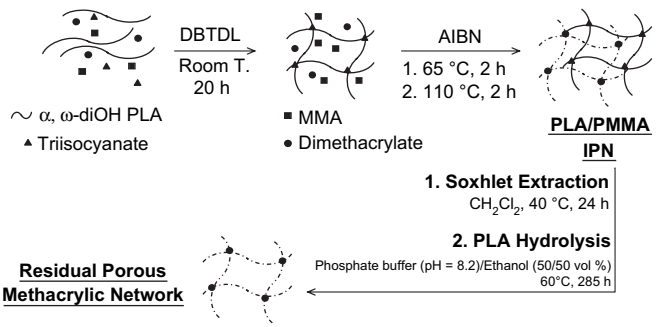

Fig. 3. Synthesis of PLA/PMMA-based IPNs and design of porous PMMA networks derived therefrom.

Larmor frequency of 75.46 MHz on a Bruker Avance 300 spectrometer using the combined techniques of cross-polarization (CP), dipolar decoupling (DD), and magic angle spinning (MAS). A 4 mm MAS head probe was used with a spinning frequency of 6500 Hz. The spectra were calibrated by taking the ^{13}C chemical shift of the carbonyl band of α-glycine as an external reference standard (176 ppm).

The size exclusion chromatography (SEC) equipment consisted of a Spectra Physics P100 pump, two PLgel 5 μm mixed-C columns (Polymer Laboratories), and a Shodex RI 71 refractive index detector. Tetrahydrofuran (THF) was used as the eluent at a flow rate of 1 mL min^{-1}, and polystyrene standards (Polymer Laboratories) were employed for calibration.

DSC analyses were carried out with a Perkin Elmer DSC 4 calorimeter under a nitrogen atmosphere. PMMA single networks and IPNs were scanned twice from −50 °C to 200 °C. PLA single networks were heated from −50 °C to 100 °C and from −50 °C to 200 °C for the first and second scans, respectively. The heating rate was equal to 20 °C min^{-1}, and the second run was recorded after quenching. No noticeable degradation was detected under such conditions. The T_g values were measured in the second run.

Scanning electron microscopy (SEM) analyses were performed with a LEO 1530 microscope equipped with a high-vacuum (10^{-10} mmHg) Gemini column. The accelerating tensions ranged from 1 to 5 kV; two detectors (InLens and Secondary Electron) were used. Prior to analyses, the samples were cryofractured and coated with a Pd/Au alloy (4 nm) in a Cressington 208 HR sputter-coater.

2.5. Kinetic studies by real-time FTIR spectroscopy

In the kinetics studies, the FTIR spectra were recorded on a Bruker Tensor 27 DTGS spectrometer between 6500 and 450 cm^{-1} by averaging 32 consecutive scans with a resolution of 4 cm^{-1}.

In the case of PLA network, the formation was monitored through the disappearance of the N=C=O stretching absorption band at 2275 cm^{-1}. The PMMA network formation could be monitored in real-time in the near-infrared spectral region through the disappearance of the C=C−H overtone absorption band from the methacrylate groups at 6168 cm^{-1}. Prior to the analyses, the validity of the Beer–Lambert law was checked in the concentration and temperature ranges used in this work. Consequently, the band intensity was directly proportional to the monomer concentration and the conversion–time profiles could be readily derived from the FTIR spectra recorded as a function of time. Indeed, from the initial absorbance value A_0 and that at a given time A_t, the relative conversion can be determined as $p = 1 - A_t/A_0$.

The mixture of all reagents was injected into an IR cell which was built for each experiment. The cell was fixed into a solid holder that was placed in an electrical heating jacket equipped with an automatic temperature controller. The temperature of the block was constant within ±1 °C of the set temperature. In the case of PMMA single networks, a glass-window cell with a 1 mm-thick Teflon® gasket was used to record the conversion of methacrylate groups, as the corresponding overtone absorption is situated in the near-infrared. Concerning PLA single networks and IPNs, a fluorine-window cell with a 200 μm-thick Teflon® gasket was used.

2.6. Thermoporometry by DSC

In order to increase the hydrophilicity of the porous methacrylic networks and facilitate the penetration of water into their pores, the samples were first immersed in ethanol for 2 h. After this preliminary treatment, deionized water was gradually added to replace the ethanol [31]. The samples were placed for 1 h in ethanol/water mixtures of different volume compositions (70/30, 50/50, 30/70 vol%), and they were then immersed in pure water for 2 weeks. After wiping, the melting thermograms of water were recorded from −50 °C to 5 °C at a heating rate of 1 °C min^{-1}.

From such melting thermograms of water contained in the porous networks, the melting temperature (T_m) depression could be correlated to the pore diameter D_p as indicated by Eq. (1) [31–33]:

$$D_p(\mathrm{nm}) = 2\left(0.68 - \frac{32.33}{T_m - T_{m0}}\right) \quad (1)$$

where T_m and T_{m0} are the melting temperatures of confined and bulk water, respectively.

The pore size distribution dV/dR vs. D_p could be derived from the melting thermograms by using Eq. (2) [31–33]:

$$dV/dR\left(\mathrm{cm^3\ nm^{-1}\ g^{-1}}\right) = \frac{dq/dt(T_m - T_{m0})^2}{32.33\rho v m \Delta H(T)} \quad (2)$$

where dq/dt, ρ, v, m and $\Delta H(T)$ are the heat flow recovered by DSC, the water density, the heating rate, the sample mass and the melting enthalpy of water, respectively. $\Delta H(T)$ was calculated from Eq. (3) [31–33]:

$$\Delta H(T)\ \left(\mathrm{J\ g^{-1}}\right) = 332 + 11.39(T_m - T_{m0}) + 0.155(T_m - T_{m0})^2 \quad (3)$$

2.7. Determination of density values and porosity ratios

Following the procedure adopted for thermoporometry analyses, the IPN samples after hydrolysis were placed in ethanol/water mixtures, and then immersed in pure water for 2 weeks at room temperature. The equilibrium mass swelling ratio, q_w, was calculated from Eq. (4):

$$q_w = \frac{m_w}{m_d} \tag{4}$$

where m_d and m_w stand for the residual masses of the hydrolyzed samples after vacuum drying, and their wet mass after wiping, respectively.

Considering that water is a non-swelling solvent for PMMA sub-chains, the water uptake could be ascribed to the filling of pores within the porous methacrylic matrix. Therefore, the pore volume could be assessed from Eq. (5), and the apparent density, d_{app}, could be obtained from Eq. (6) [34]:

$$V_{pores}\left(cm^3\ g^{-1}\right) = \frac{1}{d_s}(q_w - 1) \tag{5}$$

$$V_{pores} = \frac{1}{d_{app}} - \frac{1}{d_{true}} \tag{6}$$

where d_s and d_{true} stand for the solvent density (water), and the true density of the PMMA matrix as determined by helium pycnometry at 25 °C, respectively. A Micromeritics Accupyc 1330 equipment was used for helium pycnometry measurements.

The values of porosity ratios (P) were then derived from Eq. (7):

$$P = 1 - \frac{d_{app}}{d_{true}} \tag{7}$$

3. Results and discussion

3.1. Preparation and characterization of single networks

Before assembling PLA and PMMA into an IPN structure, PLA- and PMMA-based single networks were prepared as model systems.

3.1.1. PLA single network

First, a PLA-derivatized single network was synthesized by an end-linking reaction involving the terminal hydroxyl groups of a dihydroxy-telechelic PLA oligomer and the antagonist isocyanate functions of a trifunctional cross-linker (Desmodur® RU): polar and rigid urethane-type cross-links were thus created within the resulting network (Fig. 1). The reaction was carried out under inert atmosphere, in the presence of DBTDL as a catalyst. After 20 h at room temperature, the reaction medium was heated to 65 °C for 2 h, and finally cured at 110 °C for 2 h to ensure the completion of the cross-linking process. It is noteworthy that an isothermal thermogravimetric analysis (TGA) of the network at 110 °C for 2 h did not show any thermal degradation; a classical TGA measurement showed that the decomposition of such a structure begins at 115 °C. In order to compare this simple system with the more complex PLA-based IPNs, the formation of PLA network was conducted in dichloromethane solution with the same mass composition as that associated with IPN components, namely (PLA + Desmodur® RU)/CH_2Cl_2 was equal to 50/50 wt%.

The resulting network was subjected to a CH_2Cl_2 Soxhlet extraction for 24 h at 40 °C. As expected, the PLA single network was transparent, before and after extraction; the amount of sol fraction was 6 wt%, indicating a near completion of the cross-linking process. The FTIR spectrum showed that neither residual isocyanate functions nor hydroxyl groups (from potential dangling chains) remained in the resultant network.

The T_g value of PLA single network ranged from 20 °C ($T_{g,onset}$) to 45 °C ($T_{g,end}$), and as expected, was higher than that of the PLA oligomer precursor (15 °C), due to the rigidifying effect of the aromatic cross-links incorporated into the network structure.

3.1.2. PMMA single networks

As previously described [28], PMMA-based single networks were produced by bulk free-radical copolymerization of MMA with a dimethacrylate using AIBN as the initiator, at 65 °C for 2 h, followed by a 2 h curing process at 110 °C. Two difunctional cross-linkers with initial concentrations varying from 1 to 10 mol% were used: BADMA, a "rigid" dimethacrylate, and DUDMA, a more flexible one (Fig. 2). All networks were transparent, before and after CH_2Cl_2 extraction for 24 h at 40 °C; the amounts of sol fractions were below 5 wt%, suggesting a near completion of the cross-linking processes.

The T_g values of all extracted single networks as determined by DSC are listed in Table 1. As reported previously [28b], hardly any variation of the T_g ranges with the DUDMA content was noticed because the rigidifying effect of cross-linking might be offset by the relative flexibility of the spacer between the two methacrylate groups in DUDMA structure. Nevertheless, concerning BADMA-derivatized networks, a higher dimethacrylate content was associated with both a decrease of the T_g onset and a dramatic broadening of the T_g range.

3.2. Synthesis and characterization of PLA/PMMA IPNs

Miscellaneous IPNs constituted of PLA and PMMA sub-networks (50/50 wt%) were synthesized by the *in situ* sequential method, *i.e.* by mixing all the precursors homogeneously, and then forming both networks *via* two successive and independent cross-linking mechanisms. Hence, the PLA sub-network was first generated at room temperature for 20 h by reacting dihydroxy-telechelic PLA oligomers with Desmodur® RU *via* a DBTDL-catalyzed end-linking reaction. Subsequently, the methacrylic sub-network was created at 65 °C (2 h) by AIBN-initiated copolymerization of MMA and a dimethacrylate (BADMA or DUDMA) with varying

Table 1
DSC analysis of PLA[a] and PMMA single networks as well as PLA/PMMA (50/50 wt%) IPNs

Initial MMA/dimethacrylate composition (mol%)	Single network after extraction			IPN after extraction			IPN after hydrolysis		
	$T_{g,onset}$[b] (°C)	ΔT_g[c] (°C)	ΔC_p[d] (J g^{-1} °C^{-1})	$T_{g,onset}$[b] (°C)	ΔT_g[c] (°C)	ΔC_p[d] (J g^{-1} °C^{-1})	$T_{g,onset}$[b] (°C)	ΔT_g[c] (°C)	ΔC_p[d] (J g^{-1} °C^{-1})
MMA/BADMA									
90/10	76	90	0.12	40	30	0.18	110	54	0.19
95/5	114	54	0.20	42	28	0.17	114	48	0.23
97/3	116	29	0.20	46	30	0.22	133	37	0.15
99/1	119	18	0.24	48	24	0.28	105	39	0.17
MMA/DUDMA									
90/10	118	19	0.16	45	46	0.22	110	26	0.21
95/5	114	16	0.16	50	36	0.26	110	25	0.15
97/3	110	23	0.19	55	35	0.26	110	16	0.16
99/1	111	23	0.21	50	25	0.27	117	11	0.17

[a] PLA single network: $T_{g,onset} = 20$ °C, $\Delta T_g = 25$ °C, $\Delta C_p = 0.29$ J g^{-1} °C^{-1}.
[b] $T_{g,onset}$: value associated with the intercept of tangent to midpoint of the specific heat increment with "glassy" baseline.
[c] $\Delta T_g = T_{g,end} - T_{g,onset}$: width of glass transition range, where $T_{g,end}$ is the value associated with the intercept of tangent to midpoint of the specific heat increment with the "viscous" baseline.
[d] $\Delta C_p = C_{p,v} - C_{p,g}$: heat capacity jump at T_g, where C_p is the heat capacity, the subscripts 'v' and 'g' refer to the "viscous" and "glassy" states, respectively.

compositions, and the reaction medium was finally cured at 110 °C for 2 h to ensure a near completion of the cross-linking processes (Fig. 3). It should be stressed that Tabka and Widmaier showed that both types of cross-linking mechanisms (*i.e.* end-linking reaction catalyzed by a tin (IV) derivative and free-radical polymerization initiated by AIBN) do not interfere, while the use of AIBN in conjunction with tin(II) octanoate leads to a complex formation which substantially affects the kinetics of network formation [35]. The question that may also arise concerns the potential formation of allophanate-type bonds between both PLA and PMMA sub-networks when using the urethane-containing dimethacrylate (DUDMA). Hence, as a blank experiment, a PLA network was generated in the presence of DUDMA: after a dichloromethane Soxhlet extraction, the whole initial amount of DUDMA was removed from the polyester network, thus demonstrating that the urethane bonds within DUDMA structure did not react with the isocyanate functions from Desmodur® RU.

It is noteworthy that all IPN samples were transparent, before and after extraction in a Soxhlet reactor with CH_2Cl_2 for 24 h. Considering that the difference between the refractive indices of both IPN components is significant (n_D^{25} (PLA) = 1.51 and n_D^{25} (PMMA) = 1.49), the transparency suggested a good degree of chain interpenetration associated with both sub-networks, and was at least indicative of microdomain sizes smaller than about 150 nm [36]. Interestingly, Vancaeyzeele et al. have recently obtained similar results with polyisobutene (PIB)/PMMA [37a] and PIB/PS [37b] IPN systems, and have shown that the sub-network formation order has a significant impact on the IPN morphology and chain interpenetration. Indeed, transparent samples with the highest degree of interpenetration were produced by forming the "soft" PIB sub-network first, while opaque samples with a large phase separation were derived from a synthetic strategy involving the formation of the "rigid" sub-network first. Whatever be the dimethacrylate nature and concentration, all synthesized IPNs contained extractable contents lower than 10–12 wt%, which nearly matched the total amounts of the sol fractions encountered for PLA and PMMA single networks. Moreover, no residual hydroxyl groups were detected in the FTIR spectra of the extracted networks, suggesting the absence of any dangling chain within these structures.

3.3. Kinetic monitoring of network formation by real-time FTIR

Jin et al. have investigated the kinetics of formation associated with polyurethane (PUR)/PMMA-based IPNs by FTIR spectroscopy: the disappearance of the isocyanate stretching band at 2275 cm^{-1} was monitored for the PUR sub-network [38], while the variation of C=C stretching band at 1639 cm^{-1} was followed for the PMMA sub-network [39]. In our investigation, the C=C absorption band from the methacrylic monomers at 1640 cm^{-1} mostly overlapped the strong and relatively broad C=O stretching bands from both PMMA and PLA. Accordingly, to monitor the network formation kinetics, we selected a well-separated absorption band, namely the C=C–H overtone band of methacrylate groups located in the near-infrared spectral region at 6168 cm^{-1}. One such band was previously selected to determine the time dependence of the double bond conversion for the cross-linking of diethylene glycol bisallyl carbonate (CR39®) [40,41], as well as for the formation of PMMA single networks [28b], PMMA-based (semi-)IPNs [28b,37a], and PS-based IPNs [37b].

We first examined the kinetics of each cross-linking process involved in the formation of both PLA and PMMA single networks. The conversion–time profile for the PLA single network formation exhibited three main phases with distinct durations. A 4 h period first occurred up to 80% conversion, due to a quite rapid reaction between isocyanate and alcohol functions. A second stage then took place up to 20 h of reaction, during which conversion built up very slowly to 90%. The conversion finally reached a near completion upon raising the temperature to 65 °C, and then 110 °C.

On the other hand, the influence of the dimethacrylate content and nature on the kinetics of the free-radical copolymerization process involved in the formation of PMMA single networks was previously investigated in our group [28b]. As a reminder, the kinetic features confirmed that the curing process was effective enough to ensure a quantitative cross-linking in most cases, even though the curing temperature used in the formation of the networks (110 °C) was slightly lower than the T_g values.

Next in our investigation, the cross-linking processes involved in the formation of PLA/PMMA-based IPNs were monitored. Fig. 4 displays the time dependence of conversion associated with isocyanate functions and C=C double bonds for the formation of a 50/50 wt% PLA/PMMA IPN with an initial DUDMA content of 10 mol%. As expected, both polymerization processes did not interfere and proceeded sequentially: the creation of the PMMA sub-network was indeed triggered when the PLA sub-network formation reached a conversion higher than 90%. Actually, after a 20 h period at room temperature, the free-radical copolymerization was initiated by AIBN upon heating to 65 °C. After 2 h at such temperature, the curing stage at 110 °C turned out to be necessary to reach a near completion of both cross-linking processes.

3.4. Investigation of microphase separation in IPNs by DSC

The T_g values of extracted PLA/PMMA (50/50 wt%) IPNs as determined by DSC are reported in Table 1. All samples displayed single glass transition ranges located between the T_g of PLA single network (*i.e.* $T_{g,onset} = 20\ °C - T_{g,end} = 45\ °C$) and those of corresponding PMMA homologues (*i.e.* around 110–160 °C). In most of the systems, the value of T_g onset nearly corresponded to that of T_g end in the neat PLA network. This might arise from a partial reorganization of the soft PLA sub-network along with the creation of PLA-rich microdomains smaller than about 150 nm: this possible reorganization may occur during the formation of the methacrylic sub-network. As a matter of fact, the latter synthetic step was performed at 65 °C, *i.e.* above the T_g associated with the PLA sub-network first generated at room temperature. Such a peculiar behavior was previously evidenced by DSC and high-resolution solid-state ^{13}C NMR in an investigation of the solid-state organization of IPNs based on poly(methylphenylsiloxane) as the flexible partner and PMMA as the rigid one [42], their synthesis being similar to that adopted in our study. Furthermore, a higher dimethacrylate content in the IPN samples was generally associated with both a slight lowering of the values of T_g onset and a widening of the glass transition zones (ΔT_g), which may indicate a noticeable extent of compositional heterogeneity in IPNs with high dimethacrylate contents, so in turn a decrease of their chain interpenetration degree. Such a finding corroborated the clear conclusions inferred from our previous study on corresponding semi-IPN systems [28b]. Nevertheless, it is obvious that the spatial scale of phase separation was much smaller in IPNs than in corresponding semi-IPNs, especially at higher dimethacrylate contents and/or when using BADMA: all IPN systems were indeed transparent, while the turbidity of semi-IPN samples strongly depended on the dimethacrylate nature and content [28b]. Obviously enough, the microphase-separated morphology developed in PLA/PMMA IPNs not only resulted from the highly favorable dipole–dipole interactions between main-chain ester groups from PLA and side-chain ones from PMMA, but it was also due to the peculiar interlocking framework of both constitutive sub-networks.

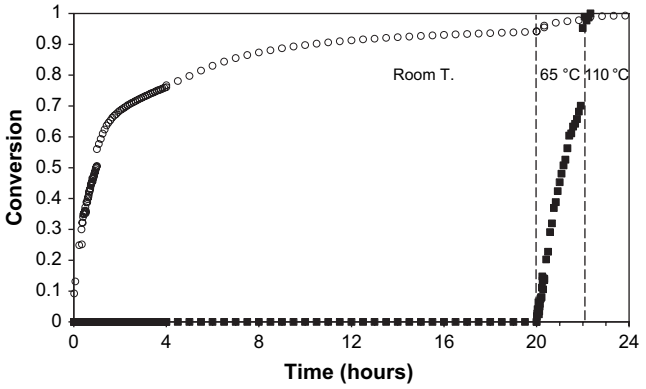

Fig. 4. Kinetic monitoring of formation of a PLA/PMMA (50/50 wt%) IPN with $[NCO]_0/[OH]_0 = 1.4$, $[DBTDL]_0/[PLA]_0 = 0.44$, $[AIBN]_0/[M]_0 = 0.02$, and an initial MMA/DUDMA composition of 90/10 mol%: (○) [NCO] conversion–time curve; (■) [C=C] conversion–time curve.

3.5. Design of porous networks from IPNs

3.5.1. Selective hydrolysis of single networks and IPNs

Advantage of the well-known hydrolytic degradability of PLA was taken to produce (meso)porous methacrylic networks with a narrow pore size distribution through the hydrolysis of the PLA sub-network associated with partially hydrolyzable PLA/PMMA IPNs. As specified in Fig. 3, this hydrolysis is conducted at 60 °C under mild conditions, namely by using a mixture of phosphate buffer (pH = 8.2) and ethanol. It has to be stressed that such a degradation was performed at a temperature intermediate between the T_g value of PLA single network (*i.e.* 20–45 °C) and that of the corresponding PMMA single networks (*i.e.* around 110–160 °C) to avoid the collapse of the residual porous methacrylic structures, while allowing for an efficient degradation of PLA. Ethanol is a good solvent of PLA oligomers, and its role was to increase the hydrophilic character of PLA/PMMA IPNs [43], thus favoring a better diffusion of the hydrolysis medium into the network structure, and accelerating the degradation rate. All extracted IPNs and the corresponding single networks as model systems were subjected to hydrolysis under identical conditions; the variations of mass loss were monitored as a function of the hydrolysis time (Fig. 5 as an example).

The PLA-based single network was completely degraded after 48 h. We observed a decrease of pH, due to the release of lactic acid in the hydrolysis medium. According to ^1H NMR and SEC analyses, the degradation products were constituted of PLA precursor, smaller oligolactides ($M_n \approx 650\ g\ mol^{-1}$,

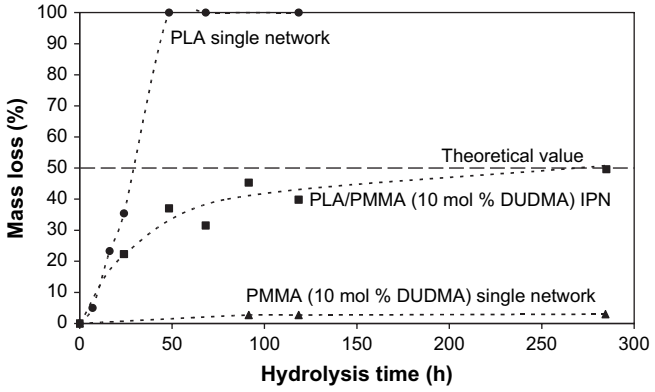

Fig. 5. Dependence of mass loss on hydrolysis time for typical network systems.

$M_w/M_n \approx 2.5$), lactic acid, and cross-linker residues, indicating that the hydrolysis affected both ester and urethane functions.

To understand how the conditions selected for PLA degradation might affect the structure of PMMA sub-networks during the partial hydrolysis of IPNs, the corresponding PMMA-based single networks were analyzed after undergoing the same experimental conditions. Mass loss increased significantly when decreasing the cross-linker content (Table 2): negligible values were found for the 10 mol% dimethacrylate-containing samples, whereas values as high as 25 wt% were assessed for their 1 mol% dimethacrylate-derivatized homologues, after 285 h. Moreover, solvent uptake also increased when the dimethacrylate content decreased. The concomitant variation of both parameters therefore indicated a non-negligible degradation of PMMA networks with lower cross-linker contents, which may be attributed to the partial hydrolysis of side-chain ester groups into carboxylic acid groups, as detected by FTIR around 3600 cm^{-1} (broad and weak band due to OH stretching vibrations). It is noteworthy that this side reaction was less and less pronounced with increasing cross-link densities, probably due to a more difficult diffusion of the hydrolysis medium into such compact and hydrophobic cross-linked structures. Further, when comparing the degradative behavior of DUDMA- and BADMA-based single networks, the latter samples were more prone to degradation. No amido-acid groups were detected around 1820 cm^{-1} in the FTIR spectra of DUDMA-based single networks after hydrolysis, thus indicating that the urethane functions from DUDMA were not hydrolyzed under the experimental conditions chosen.

As to PLA/PMMA (50/50 wt%) IPN systems, the hydrolysis of the PLA partner was much slower in comparison with the PLA single network. Such a behavior just proved the protective role played by PMMA sub-networks toward their PLA homologue: the higher the dimethacryate content, the longer the period associated with the protection. Actually, the dependence of mass loss on dimethacrylate nature and content followed the same trend as that observed for PMMA-based single networks (Table 2). Mass loss values higher than or equal to 50 wt%, *i.e.* the initial PLA mass fraction, were reached after 285 h: such values strongly suggested the

Table 2
Mass loss (Δm) and solvent uptake (Q_s) values associated with PMMA single networks and PLA/PMMA (50/50 wt%) IPNs[a]

Initial MMA/dimethacrylate composition (mol%)	Single network		IPN	
	Δm[b] (wt%)	Q_s[c] (wt%)	Δm[b] (wt%)	Q_s[c] (wt%)
MMA/BADMA				
90/10	1	84	53	167
95/5	8	126	60	200
97/3	14	165	64	260
99/1	25	249	77	433
MMA/DUDMA				
90/10	2	99	50	122
95/5	4	135	59	152
97/3	6	150	64	167
99/1	17	183	68	410

[a] Hydrolysis conditions: phosphate buffer (pH = 8.2)/ethanol (50/50 vol%), $T = 60$ °C, $t = 285$ h.

[b] $\Delta m = (m_0 - m_d)/m_0 \times 100$ where m_0 and m_d stand for the initial mass of the sample and the mass of the residual network after vacuum drying, respectively.

[c] $Q_s = (m_w - m_d)/m_d \times 100$ where m_w and m_d stand for the wet mass of the residual network just after wiping and its mass after vacuum drying, respectively.

quantitative hydrolysis of PLA sub-network along with a partial degradation of PMMA sub-networks, especially with lower cross-linker contents, as mentioned above. The maximum degradation time (285 h) was maintained constant so that all the systems might undergo identical hydrolysis conditions. The total disappearance of the characteristic bands associated with the PLA component (urethane and carbonyl groups) in FTIR and solid-state ^{13}C NMR spectra of residual networks confirmed their pure methacrylic structure. As typical examples, Fig. 6 shows the solid-state ^{13}C NMR spectra of the 1 mol% DUDMA-containing IPN samples before and after hydrolysis, as well as those of the corresponding PLA and PMMA single networks (after extraction) as model systems. The spectrum of the IPN after hydrolysis (Fig. 6d) clearly matched that of the corresponding PMMA single network (Fig. 6b). Furthermore, the T_g values of IPNs with higher cross-linker contents, after hydrolysis, were quite close to those of the corresponding PMMA single networks (Table 1). However, for systems with lower cross-linker contents, especially those containing BADMA, the T_g values of "hydrolyzed" IPNs were much higher than those of the corresponding methacrylic single networks. This noticeable increase of T_g most probably resulted from the partial hydrolysis of side-chain ester groups into carboxylic acid functions in PMMA sub-networks with lower cross-link densities, as discussed above.

3.5.2. Morphological analysis of porous networks

The morphologies of IPNs, before and after hydrolysis, were examined by SEM (Fig. 7 as typical examples). Whatever be the dimethacrylate nature and content, the non-degraded samples exhibited compact and non-porous structures (Fig. 7a and b). The corresponding PMMA single networks, after undergoing the hydrolysis conditions aforementioned, did not display any pore either, indicating a high compacity in this type of networks.

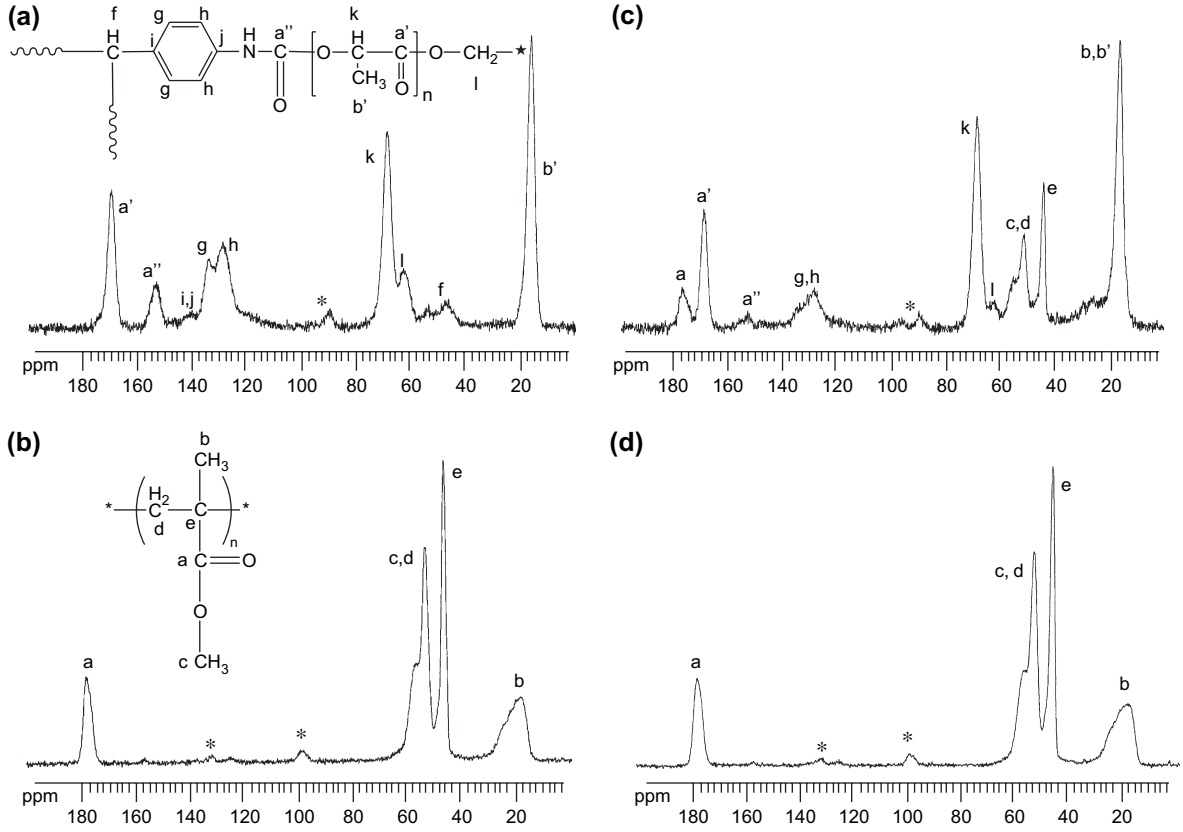

Fig. 6. Solid-state ^{13}C NMR spectra of (a) PLA single network (after extraction) and systems with an initial MMA/DUDMA composition of 99/1 mol%; (b) PMMA single network (after extraction); (c) PLA/PMMA (50/50 wt%) IPN before hydrolysis and (d) residual methacrylic network after complete PLA hydrolysis (285 h) from PLA/PMMA (50/50 wt%) IPN (the signals marked with an asterisk are assigned to spinning side bands).

However, in the case of the 1 mol% dimethacrylate-containing samples, cracks and/or blisters were detected for single networks as well as IPN systems after hydrolysis. Such damages of networks showed the fragility of the latter samples with the lowest cross-linker content, and likely originated from the partial hydrolysis of PMMA side-chain ester groups along with the generation of small molecules, such as methanol. These molecules may indeed accumulate within microcavities which constitute osmotic cracking nucleation centers [44]. After complete PLA hydrolysis from IPN precursors (285 h), the morphology exhibited by the residual methacrylic networks differed sharply from that of the corresponding single networks, despite a similar chemical structure. They revealed porous structures with pore diameters ranging from 10 to 100 nm for the 10 mol% BADMA-containing system and from 10 to 60 nm from its DUDMA-derivatized homologue, thus showing the effective role of cross-linked PLA sub-chains as porogen templates. Pore sizes decreased barely or even not at all when decreasing the dimethacrylate content (Table 3). It is noteworthy that such a dependence of pore sizes on cross-linker nature and content was dramatically different from the variation found for the corresponding semi-IPN systems [28b]. As a reminder, the pore sizes in the latter materials could be tuned within a wide range by playing on the dimethacrylate nature and content through the variation of miscibility between un-cross-linked PLA sub-chains and PMMA sub-networks in semi-IPN precursors. In particular, mesoporous networks could only be generated from the 1 mol% dimethacrylate-containing PLA/PMMA semi-IPNs characterized by a high extent of miscibility between both partners. The original approach involving the use of PLA/PMMA IPNs with higher dimethacrylate contents may therefore provide an alternative route to mesoporous cross-linked materials.

Moreover, as SEM is not a very precise technique to determine pore sizes smaller than a few tens of nanometers, we also determined pore sizes by thermoporometry through DSC analyses using water as the penetrant solvent (cf. Section 2, Eqs. (1) and (2)). Thermoporometry is a quantitative and sensitive technique allowing for the precise determination of pore size distributions in a large variety of (meso)porous materials, provided pore diameters are smaller than about 200–300 nm. It relies on the melting temperature depression and the Gibbs–Thompson effect shown by the solvent constrained within the pores [31–33]. The pore diameter ranges thus obtained are listed in Table 3, and examples of pore size distributions are presented in Fig. 8. Regardless of the dimethacrylate nature and content, relatively narrow pore size distributions were clearly observed. In addition, little – if any – variation was noticed when varying the cross-linker nature or content. One such dependence of the pore sizes and their distributions on dimethacrylate nature and content in the nanoporous networks derived from the IPN systems considered actually mirrored

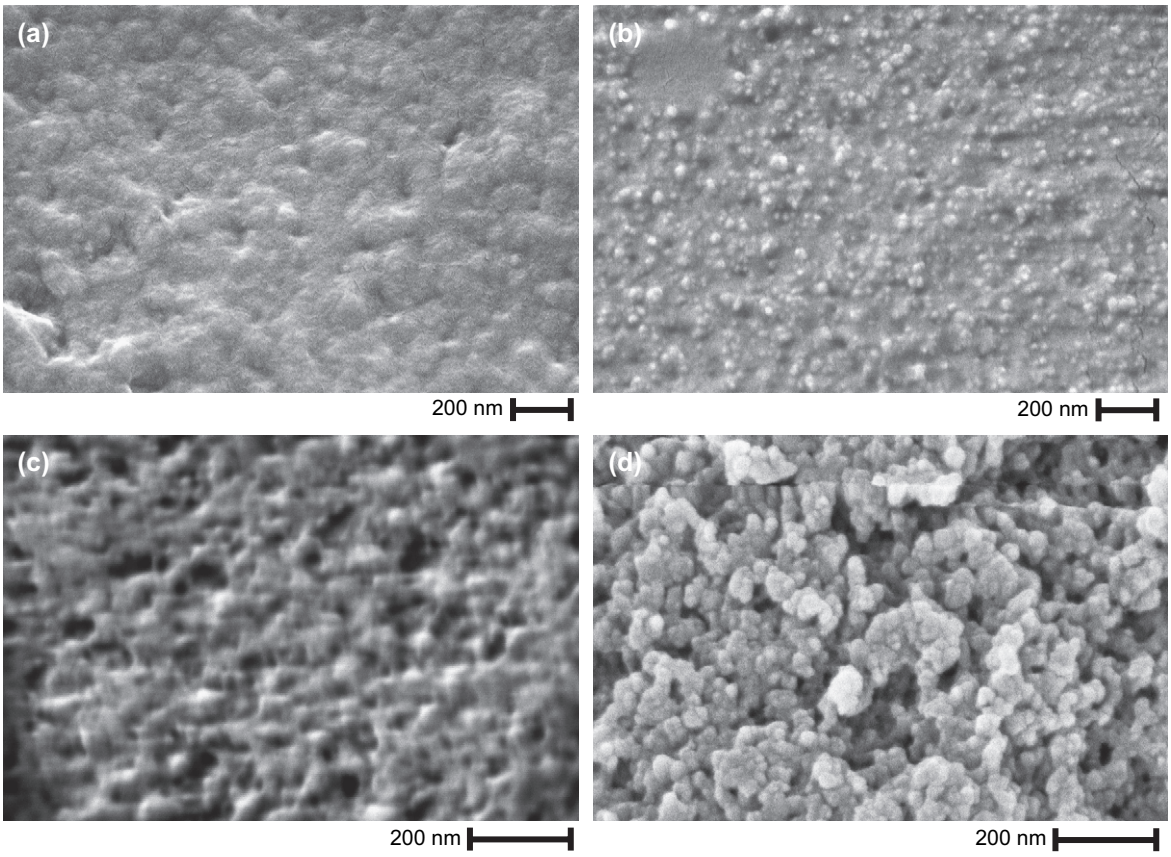

Fig. 7. SEM micrographs of different PLA/PMMA (50/50 wt%) IPN systems: before hydrolysis: (a) 10 mol% DUDMA-based sample; (b) 10 mol% BADMA-based sample; after complete PLA hydrolysis (285 h); (c) 10 mol% DUDMA-based sample and (d) 10 mol% BADMA-based sample.

the high degree of chain interpenetration and small microdomain sizes in IPN precursors, as inferred from their transparency and DSC analyses.

3.5.3. Evaluation of apparent density and porosity ratio

After total PLA hydrolysis from IPN precursors (285 h), the pore volumes (V_{pores}) of the residual methacrylic networks were determined through measurements of equilibrium mass swelling ratios in water, which allowed for the evaluation of apparent density (d_{app}) and porosity ratio (P) values (cf. Section 2, Eqs. (4)–(7)). The experimental values related to V_{pores}, true density (d_{true}), d_{app}, and P are given in Table 4. Interestingly, the true density values of porous networks were very close to those of corresponding methacrylic single networks. For instance, after complete PLA hydrolysis (285 h), the 10 and

Table 3
Pore diameters of resulting porous networks as determined by SEM and thermoporometry after complete PLA hydrolysis from PLA/PMMA (50/50 wt%) IPNs[a]

Initial MMA/dimethacrylate composition (mol%)	Pore diameter SEM (nm)	Pore diameter thermoporometry (nm)
MMA/BADMA		
90/10	10–100	30–100
95/5	10–50	15–60
97/3	10–50	15–60
99/1	10–50	15–50
MMA/DUDMA		
90/10	10–60	20–80
95/5	10–50	15–60
97/3	10–50	15–55
99/1	10–50	15–50

[a] Hydrolysis conditions: phosphate buffer (pH = 8.2)/ethanol (50/50 vol%), $T = 60$ °C, $t = 285$ h.

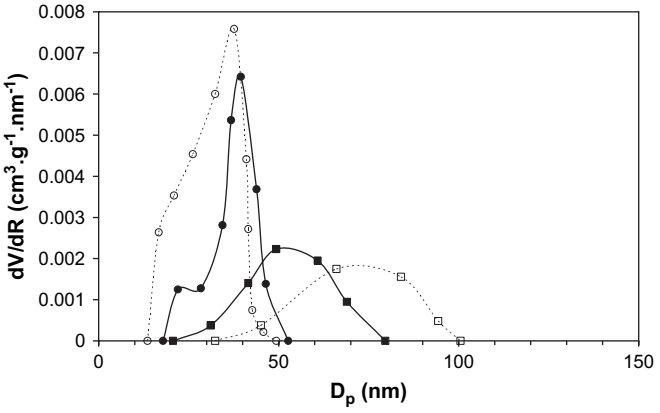

Fig. 8. Pore size distribution profiles of porous methacrylic networks resulting from PLA hydrolysis (285 h) in PLA/PMMA (50/50 wt%) IPNs as determined by thermoporometry for DUDMA- (full symbols) and BADMA-containing (empty symbols) systems with different initial MMA/dimethacrylate compositions: (■, □) 90/10 mol%; (●, ○) 99/1 mol%.

Table 4
Values of pore volume (V_{pores}), true density (d_{true}), apparent density (d_{app}) and porosity ratio (P) of resulting porous networks after complete PLA hydrolysis from PLA/PMMA (50/50 wt%) IPNs[a]

Initial MMA/dimethacrylate composition (mol%)	BADMA				DUDMA			
	V_{pores}[b] ($cm^3\ g^{-1}$)	d_{true}[c]	d_{app}[d]	P[e]	V_{pores}[b] ($cm^3\ g^{-1}$)	d_{true}[c]	d_{app}[d]	P[e]
90/10	0.56	1.194	0.72	0.40	0.55	1.204	0.72	0.40
95/5	0.59	1.179	0.70	0.41	0.61	1.175	0.68	0.42
97/3	0.71	1.167	0.64	0.45	0.69	1.165	0.65	0.44
99/1	0.87	1.149	0.57	0.50	0.71	1.150	0.63	0.45

[a] Hydrolysis conditions: phosphate buffer (pH = 8.2)/ethanol (50/50 vol%), $T = 60\ °C$, $t = 285$ h.
[b] $\Delta V_{pores} = \pm 0.02$.
[c] $\Delta d_{true} = \pm 0.001$.
[d] $\Delta d_{app} = \pm 0.02$.
[e] $\Delta P = \pm 0.02$.

1 mol% BADMA-containing IPN samples had d_{true} values at 25 °C equal to 1.194 and 1.149, respectively, and the values of d_{true} for the corresponding single networks were, respectively, equal to 1.198 and 1.158. Such a good match strongly suggested that the porous networks investigated were characterized by open pore structures with interconnected channels through which a fluid (helium or water) could flow.

Furthermore, porosity ratio values ranged from 0.4 to 0.5, depending on the cross-linker content. A lower dimethacrylate content in the methacrylic networks was associated with both a decrease in the apparent density and a slight increase of the porosity ratio. The side degradation of PMMA sub-networks which essentially occurred with lower cross-link densities, during the partial hydrolysis of IPNs, may account for such variations. Within experimental errors, it can be assumed that such P values were in quite good agreement with those expected, taking into account the quantitative hydrolysis of PLA sub-network from IPNs with an initial 50/50 wt% PLA/PMMA composition.

4. Conclusion

Original template-oriented routes have recently been developed to engineer nanoporous polymeric materials with a well-defined porosity. They generally entail the selective removal of single polymer domains acting as porogen templates from macromolecular architectures with controlled degradability. This contribution has expanded the scope of the use of (semi-)-IPNs as nanostructured precursors to (meso)porous cross-linked materials. The quantitative hydrolysis of the polyester sub-network from PLA/PMMA-based IPNs does constitute an effective and versatile strategy for generating mesoporous methacrylic networks. Thus, cross-linked PLA sub-chains may well serve as porogen templates for the design of such nanoporous polymers. In these systems, the relatively small pore sizes (10–100 nm at most) are controlled by the good degree of chain interpenetration in IPN precursors. The peculiar interlocking framework of both constitutive sub-networks, associated with highly favorable dipole–dipole interactions between main-chain ester groups from PLA and side-chain ones from PMMA, indeed restrict the spatial scale of phase separation to tens of nanometers domain sizes. The transparency of PLA/PMMA IPNs and DSC investigation of their microphase separation gave evidence of the latter assertion.

The two approaches that we have envisioned so far for engineering mesoporous networks involve the use of either PLA/PMMA-based semi-IPNs or the corresponding IPNs. The first approach applying the extraction of un-cross-linked oligoesters from PLA/PMMA-based semi-IPNs constitute a straightforward and effective methodology, provided the extent of miscibility between both partners is high, *i.e.* when using the 1 mol% dimethacrylate-containing samples (DUDMA-based system preferentially) [28b]. Alternately, the second strategy implying the utilization of PLA/PMMA-based IPNs offers more versatility, since mesoporous polymers can be obtained with a wide range of dimethacrylate contents (nearly up to 10 mol%), regardless of their nature. The influence of the oligoester nature and molar mass in (semi-)IPNs on the porosity associated with the porous networks derived therefrom will be published in a forthcoming paper.

These complementary approaches involving semi-IPN and IPN systems may provide an interesting means to tune the morphology and functionality associated with porous scaffolds. The potential applications of such functional porous materials are mainly expected in the areas of separation techniques (chromatographic supports), as well as chemistry in confined media (nanoreactors).

Acknowledgements

The “Région Ile-de-France” Council is gratefully acknowledged for financial support through SESAME projects allowing for the purchase of SEM and solid-state NMR equipments. The authors thank the French Ministry of Research for providing G.R. with a grant. They are also indebted to Dr. C. Lorthioir for stimulating discussions on the characterization of networks, C. Gaillet for her kind assistance in performing solid-state NMR analyses, as well as Dr. J.L. Pastol and A. Valette (CNRS, Vitry-sur-Seine, France) for their cooperation in SEM analyses.

References

[1] Odani H, Masuda T. Design of polymer membranes for gas separation. New York: VCH; 1992.
[2] Maier G. Angew Chem Int Ed 1998;37:2960.
[3] Buchmeiser MR. Angew Chem Int Ed 2001;40:3795.
[4] Svec F, Peters EC, Sykora D, Yu C, Fréchet JMJ. J High Resolut Chromatogr 2000;23:3.
[5] Martin CR. Science 1994;266:1961.
[6] Koros WJ, Fleming GK, Jordan SM, Kim TH, Hoelm HH. Prog Polym Sci 1988;13:339.
[7] Hentze H-P, Antonietti M. Rev Mol Biotech 2002;90:27.
[8] Balaji R, Boileau S, Guérin Ph, Grande D. Polym News 2004;29:205.
[9] Haupt K, Mosbach K. Trends Biotechnol 1998;16:468.
[10] Wulff G. Chem Rev 2002;102:1.
[11] (a) Maki-Ontto R, de Moel K, de Odorico W, Ruokolainen J, Stamm M, ten Brinke G, et al. Adv Mater 2001;13:117;
(b) De Moel K, Alberda van Ekenstein GOR, Nijland H, Polushkin E, ten Brinke G, Maki-Ontto R, et al. Chem Mater 2001;13:4583;
(c) Ikkala O, ten Brinke G. Science 2002;295:2407.

[12] (a) Lee JS, Hirao A, Nakahama S. Macromolecules 1988;21:274;
(b) Lee JS, Hirao A, Nakahama S. Macromolecules 1989;22:2602.
[13] Hashimoto T, Tsutsumi K, Funaki Y. Langmuir 1997;13:6869.
[14] (a) Park M, Harrison C, Chaikin PM, Register RA, Adamson DH. Science 1997;276:1401;
(b) Li RR, Dapkus PD, Thompson ME, Jeong WG, Harrison C, Chaikin PM, et al. Appl Phys Lett 2000;76:1689.
[15] (a) Hedrick JL, Carter KR, Richter R, Miller RD, Russell TP, Flores V, et al. Chem Mater 1998;10:39;
(b) Mansky P, DeRouchey J, Russell TP, Mays J, Pitsikalis M, Morkved T, et al. Macromolecules 1998;31:4399;
(c) Thurn-Albrecht T, DeRouchey J, Russell TP, Jaeger H. Macromolecules 2000;33:3250;
(d) Thurn-Albrecht T, Steiner R, DeRouchey J, Stafford CM, Huang E, Bal M, et al. Adv Mater 2000;12:787;
(e) Xu T, Kim HC, DeRouchey J, Seney C, Levesque C, Martin P, et al. Polymer 2001;42:9091;
(f) Goldbach JT, Russell TP, Penelle J. Macromolecules 2002;35:4271;
(g) Thurn-Albrecht T, DeRouchey J, Russell TP, Kolb R. Macromolecules 2002;35:8106;
(h) Xu T, Hawker CJ, Russell TP. Macromolecules 2003;36:6178;
(i) Goldbach JT, Lavery KA, Penelle J, Russell TP. Macromolecules 2004;37:9639.
[16] (a) Liu GJ, Ding JF, Guo A, Herfort M, Bazzett-Jones D. Macromolecules 1997;30:1851;
(b) Liu GJ, Ding JF, Hashimoto T, Kimishima K, Winnik FM, Nigam S. Chem Mater 1999;11:2233.
[17] Chan VZH, Hoffman J, Lee VY, Iatrou H, Avgeropoulos A, Hadjichristidis N, et al. Science 1999;286:1716.
[18] (a) Zalusky AS, Olayo-Valles R, Taylor CJ, Hillmyer MA. J Am Chem Soc 2001;123:1519;
(b) Zalusky AS, Olayo-Valles R, Wolf JH, Hillmyer MA. J Am Chem Soc 2002;124:12761;
(c) Cavicchi KA, Zalusky AS, Hillmyer MA, Lodge TP. Macromol Rapid Commun 2004;25:704;
(d) Rzayev J, Hillmyer MA. Macromolecules 2005;38:3;
(e) Mao H, Hillmyer MA. Macromolecules 2005;38:4038;
(f) Hillmyer MA. Adv Polym Sci 2005;190:137;
(g) Mao H, Hillmyer MA. Soft Matter 2006;2:57.
[19] Li M, Douki K, Goto K, Li X, Coenjarts C, Smilgies DM, et al. Chem Mater 2004;16:3800.
[20] Uehara H, Yoshida T, Kakiage M, Yamanobe T, Komoto T, Nomura K, et al. Macromolecules 2006;39:3971.
[21] (a) Hedrick JL, Miller RD, Hawker CJ, Carter KR, Volksen W, Yoon DY, et al. Adv Mater 1998;10:1049;
(b) Hedrick JL, Carter KR, Labadie JW, Miller RD, Volksen W, Hawker CJ, et al. Adv Polym Sci 1999;141:1;
(c) Nguyen C, Hawker CJ, Miller RD, Huang E, Hedrick JL, Gauderon R, et al. Macromolecules 2000;33:4281.
[22] Eigner M, Voit B, Estel K, Bartha JW. e-Polymers 2002:028.
[23] Loera AG, Cara F, Dumon M, Pascault JP. Macromolecules 2002; 35:6291.
[24] (a) Widmaier JM, Sperling LH. Macromolecules 1982;15:625;
(b) Widmaier JM, Sperling LH. Br Polym J 1984;16:46.
[25] Du Prez F, Goethals EJ. Macromol Chem Phys 1995;196:903.
[26] (a) Hu J, Pompe G, Schulze U, Pionteck J. Polym Adv Technol 1998; 9:746;
(b) Hu J, Schulze U, Pionteck J. Polymer 1999;40:5279;
(c) Pionteck J, Hu J, Schulze U. J Appl Polym Sci 2003;89:1976.
[27] (a) Sperling LH. Interpenetrating polymer networks and related materials. New York: Plenum Press; 1981;
(b) Klempner D, Sperling LH, Utracki LA, editors. Interpenetrating polymer networks. Advances in chemistry series, vol. 239. Washington, DC: American Chemical Society; 1994;
(c) Sperling LH, Mishra V. Polym Adv Technol 1996;7:197;
(d) Kim SC, Sperling LH, editors. IPNs around the world: science and engineering. Chichester, UK: Wiley; 1997.
[28] (a) Grande D, Pastol JL, Guérin Ph, Boileau S. Polym Prepr 2003; 44(1):44;
(b) Rohman G, Grande D, Lauprêtre F, Boileau S, Guérin Ph. Macromolecules 2005;38:7274.
[29] Djomo H, Morin A, Damyanidu M, Meyer GC. Polymer 1983;24:65.
[30] Bachari A, Bélorgey G, Hélary G, Sauvet G. Macromol Chem Phys 1995;196:411.
[31] (a) Brun M, Lallemand A, Quinson JF, Eyraud C. Thermochim Acta 1977;21:59;
(b) Quinson JF, Mameri N, Guihard N, Bariou B. J Membr Sci 1991; 58:191.
[32] Hay JN, Laity PR. Polymer 2000;41:6171.
[33] Nedelec J-M, Baba M. Recent Res Devel Physical Chem 2004;7: 381.
[34] Rabelo D, Coutinho FMB. Polym Bull 1993;30:725.
[35] (a) Tabka MT, Widmaier JM. Macromolecules 1999;32:2520;
(b) Tabka MT, Widmaier JM. Macromol Symp 2001;171:123;
(c) Tabka MT, Widmaier JM. J Appl Polym Sci 2002;85:1929.
[36] Okay O. Prog Polym Sci 2000;25:711.
[37] (a) Vancaeyzeele C, Fichet O, Boileau S, Teyssié D. Polymer 2005; 46:6888;
(b) Vancaeyzeele C, Fichet O, Laskar J, Boileau S, Teyssié D. Polymer 2006;47:2046.
[38] Jin SR, Meyer GC. Polymer 1986;27:592.
[39] Jin SR, Widmaier JM, Meyer GC. Polymer 1988;29:346.
[40] Hill DJT, O'Donnell HJ, Pomery PJ. Eur Polym J 1997;33:1353.
[41] Laskar J, Vidal F, Fichet O, Gauthier C, Teyssié D. Polymer 2004; 45:5047.
[42] Brachais L, Lauprêtre F, Caille JR, Teyssié D, Boileau S. Polymer 2002; 43:1829.
[43] Wei J, Bai XY, Yan J. Macromolecules 2003;36:4960.
[44] Gautier L, Mortaigne B, Bellenger V, Verdu J. Polymer 2000;41: 2481.